Proceedings of the 1st International Symposium on Scanning Probe Spectroscopy and Related Methods, Poznań 1997

SCANNING PROBE MICROSCOPY AND SPECTROSCOPY OF HIGH TEMPERATURE SUPERCONDUCTORS

A.L. DE LOZANNE*, H.L. EDWARDS†, C. YUAN‡ AND J.T. MARKERT

Department of Physics, University of Texas, Austin, TX 78712-1081, USA

The authors review recent studies of high temperature superconductors conducted with scanning tunneling and magnetic force microscopes. Emphasis is placed on the importance of surface and probe characterization, both of which are likely to affect the detailed nature of the observations.

PACS numbers: 61.16.Ch, 74.50.+r, 07.79.Cz, 07.79.Pk, 74.72.Bk, 74.72.Hs

1. Introduction

Tunneling spectroscopy has been a very powerful tool for the study of the electronic properties of metals and semiconductors for several decades [1]. Traditionally this was done by tunneling through a thin insulator between two electrodes (a "sandwich" geometry). The advent of the scanning tunneling microscope (STM) was therefore very exciting because it opened the possibility of doing spectroscopic measurements using a vacuum gap as a tunneling barrier. This meant that more materials could be studied because many materials do not form a good native oxide or cannot be covered with a deposited thin film ("artificial") barrier. Vacuum is the ideal tunneling barrier. Furthermore, the STM also made it possible to do these spectroscopic measurements with unprecedented spatial resolution, down to the atomic scale. Some of this promise has been fulfilled over the last decade, particularly on semiconductor surfaces [2, 3]. In this invited paper the authors review the use of the STM and of the magnetic force microscope (MFM) to study superconductors, while an overall review of the beginning of the STM field has been given elsewhere [4]. For the sake of brevity this is not a comprehensive review, but only a compilation of highlights from the authors' laboratory.

The exquisite spatial and spectroscopic resolution of the STM unfortunately means that it is sensitive to the detailed atomic configuration of both the tip and the sample, so that a given measurement may not be characteristic of the material being studied, but only a result of the particular state of the tip and/or the sample.

*To whom all correspondence should be addressed (Lozanne@physics.utexas.edu).
†Present address: MS 147, PO Box 655936, Texas Instruments, Dallas, TX 75265, USA.
‡Present address: MS 30, PO Box 83180, Wacker Siltronic, Portland, OR 97283-0180, USA.

It is therefore very important to do as much characterization of the tip and the sample in order to gain confidence on these measurements. This is discussed in some detail.

2. STM of superconductors

The first low temperature STM (LT STM) was built by the first author and coworkers [5, 6] with the explicit goal of studying superconductors. The highest superconducting transition temperature (T_c) at that time was in the A-15 materials, of which Nb_3Sn is a classic example with $T_c = 18$ K. They were able to observe the superconducting gap of this compound and how it varied on the surface [5, 6].

Soon after the discovery of a higher T_c in the perovskite compound $La_{1-x}Sr_xCuO_{4-y}$, the first author and coworkers used a second generation LT STM to observe its gap [7], yielding a rather large value ($\Delta = 12$ mV, or a ratio $2\Delta/kT_c = 7$, which is twice as large as that expected from BCS theory). This was the first report of such a measurement on the high T_c superconductors. The first samples of these new materials were pressed ceramic pellets with very rough surfaces, so that it was not possible to obtain STM images of the surface or a reasonable spatial mapping of the gap. The best images were obtained later by using thin film samples [8], in this case of $YBa_2Cu_3O_{7-x}$, but even when making the samples immediately before transferring to the LT STM, the spectroscopic measurements did not show a superconducting gap reproducibly. A substantial amount of effort was spent on this, since a transfer vessel was developed to keep the samples in pure oxygen while being transported from the deposition chamber to the LT STM chamber [8].

The only method that our group has found to work reliably to prepare a good surface of $YBa_2Cu_3O_{7-x}$ is to cleave the sample in the LT STM at temperatures below 30 K, without warming the sample after cleaving. This means that the STM tip has to be lined up with the freshly cleaved surface *in situ* at low temperature, which is not trivial because the samples are 0.5–0.7 mm in diameter. This is possible because this LT STM has windows for viewing the whole STM. These windows have heat-absorbing glass to avoid warming up the STM. More experimental details of the STM and the sample mounting and cleaving are given in Refs. [9] and [10].

Such a freshly cleaved surface will show the CuO chain layer and the BaO layer. An example of the former is shown in Fig. 1. The diagonal lines are the CuO chains of this compound, which were well known from X-ray studies but had never before been imaged in real space. The image shows that the distance between chains is 0.4 nm, which agrees with the X-ray data within the resolution of the STM, but the distance between maxima along the chain, about 1.3 nm, is longer than expected. The chains are aligned along the b-axis of the unit cell, which has a repeat distance of 0.4 nm (the a and b axes of the unit cell are slightly different, but this difference is too small for the STM to distinguish), so the observed distance between bumps along the chain is about three times the length of the unit cell. The behavior of these maxima along the chain when the tunneling direction is reversed is a hint that a charge density wave may be present in the chains [11, 12]. More recently, evidence for a 1.66-nm modulation along the chains has been observed by

Fig. 1

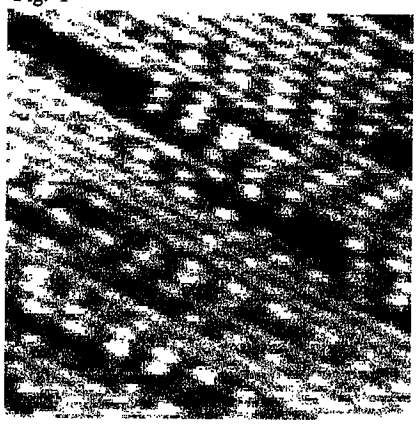

Fig. 2

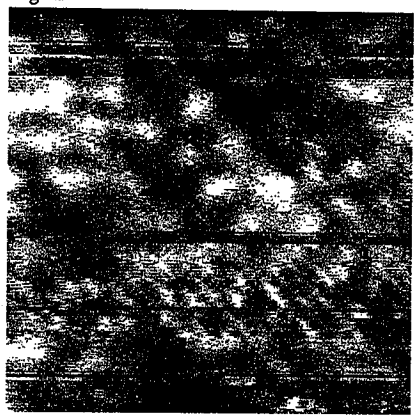

Fig. 1. STM image, 10 nm on a side, taken at 20 K with +240 mV sample bias and 40 pA tunneling current. The diagonal lines from upper left to lower right are the CuO chains of YBCO. The large depressions are due to oxygen vacancies. Reproduced from Ref. [11].

Fig. 2. STM topographic image (+300 mV sample bias, 200 pA) taken simultaneously with the spectroscopic CITS data shown in Figs. 3 and 4. All images are 10 nm×10 nm. The image quality is worse than normal because a full $I-V$ curve is taken at a grid of 128 × 128 points simultaneously with this image, and the whole process takes 2 hours. Reproduced from Refs. [9] and [16].

neutron diffraction [13], which is a bulk measurement, thus confirming the STM observations and establishing that this is not just a surface phenomenon. The slight difference in the periods measured by the two techniques is likely due to the different electronic environment for the chains on the surface compared to those in the bulk.

The spectroscopy on this surface was first done with an analog circuit [14]. More recently a commercial electronics system was used to acquire a large amount of data using a technique called current imaging tunneling spectroscopy (CITS) [2]. This consists of taking a standard topographic STM image, but stopping the scan at a predetermined grid of points, disengaging the feedback loop and sweeping the voltage while recording the current. In the case of the data shown in Fig. 2, the STM image has 256×256 points, while the spectroscopic data (Fig. 3) was recorded on a matrix of 128 × 128 points, with 32 points on each $I-V$ curve. Since this is a very large amount of data it takes 2 hours to finish such a CITS scan, so that some thermal drift (about 2 nm) is observed during the process. This is actually a very small amount of drift for such a long time of data acquisition, and is due to good thermal stability and the fact that the expansion coefficients of most materials go to zero at low temperatures. Nevertheless, the strength of CITS is that the topographic image and the spectroscopic data are strictly correlated because they are taken simultaneously. It is also possible to do simultaneous spectroscopic and topographic scans in an analog fashion by biasing the STM junction with an ac

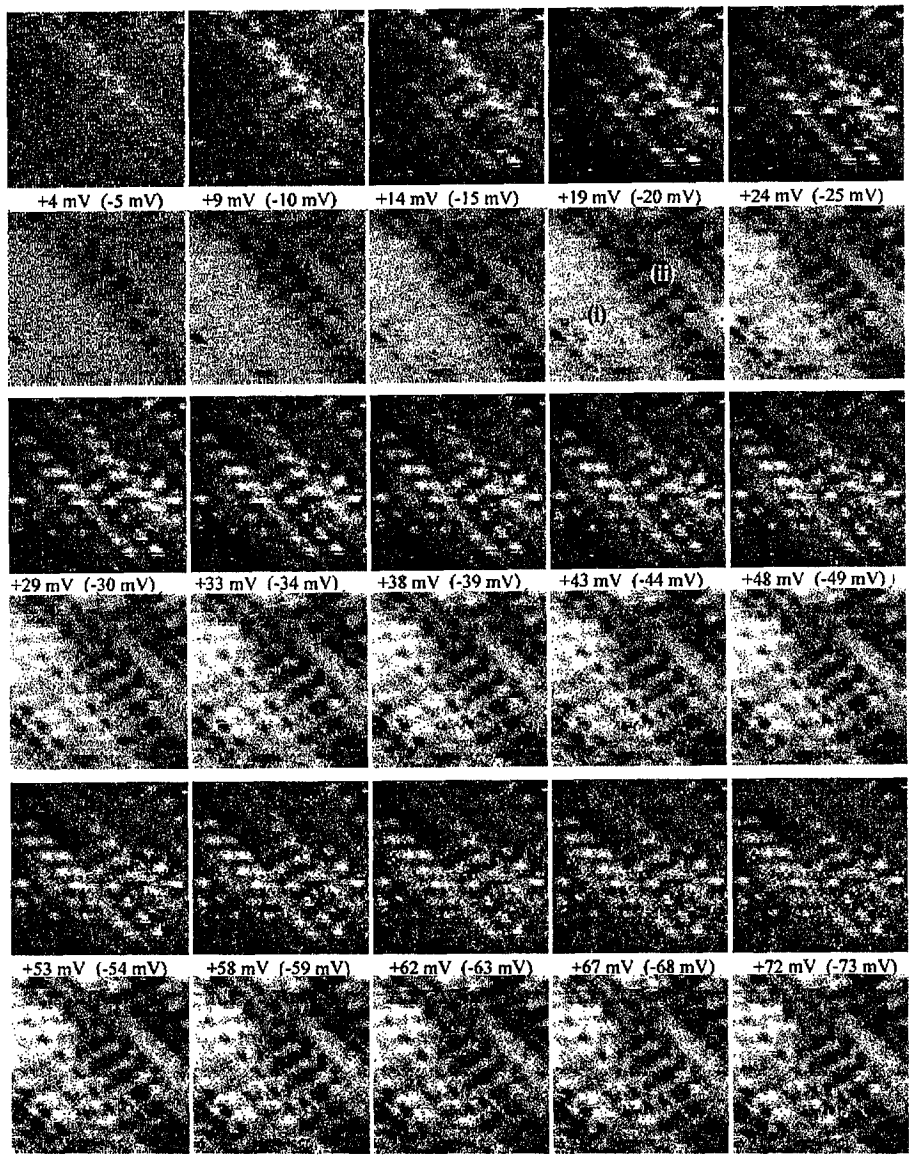

Fig. 3. Current (not topographic) images taken simultaneously with Fig. 2. The positive (negative) sample bias, in millivolts, is for the image above (below) the label. Reproduced from Refs. [9] and [16].

voltage signal (essentially scanning a full $I-V$ curve continuously) and feeding the whole ac current signal to a lock-in amplifier [5]. The output of the lock-in is the average resistance of the junction, which can be used as a feedback signal to maintain a constant distance from the surface while scanning (neglecting details of changes of electronic properties or "work function").

An important point to emphasize about the small images in Fig. 3 is that these are not STM images, or "topography", loosely speaking. It is easy to be confused because they look like STM topographic images, but actually they represent a spatial map of the current at a particular voltage. An STM image, on the other hand, is a map of the tip height required to maintain a desired fixed current at the specified tunneling voltage, which turns out to be contours of equal density of states of the sample [15]. If one studies these CITS images for the voltages near zero bias and up to just above the gap (±30 mV), one can see that a gap must be present in the lower left corner because that area is featureless for low voltages. This makes sense because inside the gap there is very little current available, yielding no current contrast as a function of position. The upper right, on the other hand, develops features even at the lowest voltages, indicating that there is no gap in this region. This is more dramatically seen by subtracting current images taken at neighboring voltages (which is an approximation to the conductance $\mathrm{d}I/\mathrm{d}V \approx \Delta I/\Delta V$) and normalizing by the overall resistance, which results in a logarithmic conductance $(\mathrm{d}(\log I)/\mathrm{d}(\log V) = (\mathrm{d}I/\mathrm{d}V)/(I/V))$. These operations are done point by point with two neighboring current images. The result is shown in Fig. 4 for the pair taken at −25 mV and −20 mV. The bright areas in this logarithmic conductance map immediately reveal to the eye the regions that have a gap, while the dark areas have no gap. This can be confirmed by looking at individual $I-V$ curves, as is shown in Fig. 5. This is therefore a very powerful technique for studying the spatial variations of superconductivity on the surface.

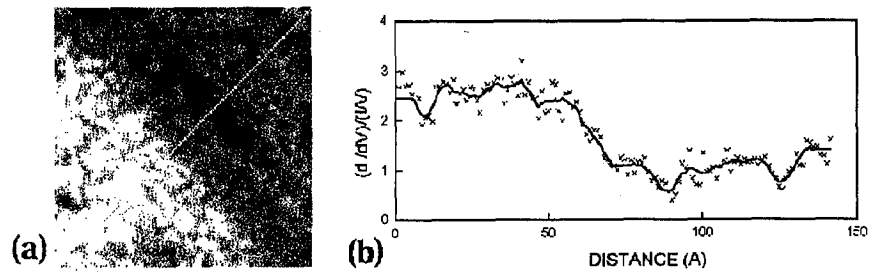

Fig. 4. Spatial map (a) of the logarithmic derivative $[\mathrm{d}I/\mathrm{d}V]/[I/V]$ at $V = -22.5$ mV, obtained by subtracting the current image (Fig. 3) at $V = -20$ mV from the one at $V = -25$ mV and dividing by the average of the two. A slight spatial averaging is done to reduce the noise introduced by taking differences. The cross-section (b) is taken through the diagonal shown in the image. The vertical scale in the cross-section is arbitrary, so we have normalized it to 1 in the normal region. Reproduced from Refs. [23] and [24].

In the past, we have associated the gapless regions with oxygen vacancies on the surface [16]. There are several depressions seen in the upper right of the topographic image which are likely to be oxygen vacancies. The simple theoretical model is that oxygen vacancies in the chains act as magnetic impurities [17], which break superconducting pairs and destroy superconductivity locally. On the other hand, the boundary between the bright and dark regions of Fig. 4 is quite straight,

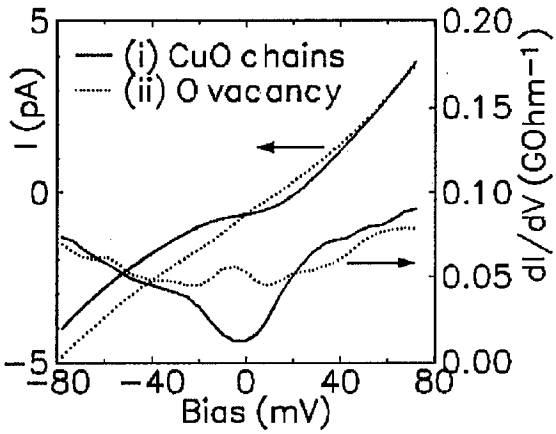

Fig. 5. Behavior away from an oxygen vacancy (labeled (i) in the -20 mV image of Fig. 5) and near the oxygen vacancy (labeled (ii) in the -20 mV image of Fig. 5). A gap is clearly observed only in the first case. Reproduced from Refs. [9] and [16].

namely it does not seem to follow the locations of the oxygen vacancies. It is possible that an alternative explanation is that the straight boundary is due to a stripe phase [18].

One final interesting conclusion to draw from this data is to estimate the coherence length, which determines the shortest distance over which superconductivity can change. In other words, any spatial variations of superconductivity have to happen over distances equal to or larger than the coherence length. Figure 4b shows a cross-section through the logarithmic conductance image in Fig. 4a, which shows a change from superconducting to non-superconducting in about 2 nm. The accepted coherence length in the a–b plane of $YBa_2Cu_3O_{7-x}$ is 1 nm, consistent with the estimate obtained from the figure.

3. The need for better characterization

The powerful capabilities of the STM and its potential for doing spectroscopy have attracted many people from the field of superconductivity. The first author was in this situation in 1982, soon after the first STM reports by Binnig, Rohrer, and Gerber [19]. Fortunately at that time STM was in its infancy, so the author had time to "grow" with the field of STM. Many of the newer groups using STM on superconductors do not have the benefit of such experience and may assign great significance to observations which could be due to artifacts. References could be given to illustrate the problems, but it would be unfair to criticize a particular publication when the problem is widespread. Also, many times the data may be suspect, but one cannot show that there is something wrong with it from reading the publication. It is up to the researcher to make sure that the data is valid, and to describe the tests that were done. This section lists some of the tests that should be done by every group, not necessarily on every data set taken, but at least on a given type of sample in order to learn the correct behavior of the STM under optimal conditions.

Most people using STM are aware that they should test their images by changing scan size, scan frequency, scan rotation and sample rotation (the difference between the latter two tests may not be evident to all researchers). Different artifacts produce different results under these tests.

Spectroscopy is more difficult to validate. Certainly the above tests should be done on the same area of the sample and the spectroscopy should be correlated to the positions on the surface. The exponential dependence of the tunneling current upon tip/sample distance should be measured and a work function should be estimated. If the work function is too low (below about 0.5 eV) the spectroscopy is suspect (so is the microscopy, but to a lesser extent). All tests should be done under conditions similar to those during data acquisition. As an example of the contrary, some groups take microscopy and work function data at a reasonable tip–sample distance (with junction resistances in the order of a gigaohm) but then let the tip come closer to the surface for the spectroscopy. For this reason the resistance or conductance of the tip–sample junction should always be given both for the microscopy as well as for the spectroscopy. Again, some groups give spectroscopy data with arbitrary units of conductance and with arbitrary shifts on the vertical scale, which is a bad practice. The fact that there is no change in the topographic images before and after spectroscopy does not validate the latter, because it is possible to elastically deform the tip/sample area during spectroscopy and therefore not affect the microscopy.

Our method for cleaving samples *in situ* at low temperatures is the best way we have found to prepare a clean surface, but this is by no means perfect. The sample can cleave through the most defective parts of the crystal, so the surface may not be representative of good material. The tip can pick up debris from the cleaved surface and, while this can produce high resolution and reproducible images, it may adversely affect the spectroscopic measurements because as the tip–sample voltage is swept, the field in the junction changes, which can make a loose particle or atom change its position and thus dramatically change the junction. As the voltage is swept back and forth the loose particle or atom can rock back and forth, thus giving a reproducible $I-V$ curve which has nothing to do with the material being studied. Depending on details, charging effects may play a role [20]. These problems are not unique to cleaved surfaces.

There is one final concern regarding the practice of allowing the tip to touch the surface for spectroscopic measurements, which is what has been done for decades before the STM and is known as point contact spectroscopy. Such a technique has worked in the past because the older superconductors had much simpler structures, with only one of two elements, simple unit cells, and longer coherence lengths. Since tunneling probes a depth on the order of a coherence length, which is of the order of a few angstroms along the c-axis of high temperature superconductors, one has to worry about the nature of the last few layers near the contact or tunneling point. If this is damaged or changed in any fashion one is not measuring the properties of the bulk superconductor. Some would argue that such measurements are valid because they are reproducible, but it is possible to move the tip in all three dimensions until a desirable $I-V$ curve is seen and recorded, while a

wide variety of other $I-V$ curves are ignored. In other words, "reproducibility" can be achieved by the operator tweaking the junction until the "right" curve is observed and recorded.

4. Low temperature magnetic force microscopy (LT MFM)

While the author's group has been successful in obtaining excellent STM data on cleaved $YBa_2Cu_3O_{7-x}$ crystals, this is a difficult and time consuming task. Consequently a more forgiving technique for imaging superconductors was developed based on the magnetic force microscope [21, 22]. The easiest way to understand why an MFM should be sensitive to superconductive properties is to remember the classic demonstration of a permanent magnet levitating above a high T_c superconductor. The Meissner effect in the superconductor expels the flux and repels the magnet. Another way to understand this is that the superconductor acts as a magnetic mirror, so the magnet is repelled by its image behind this mirror. In the case of the MFM the permanent magnet is a microscopic particle of iron or cobalt on the tip. As this microscopic magnet is scanned over the surface it is repelled over superconducting regions and not over the normal regions, thus providing contrast between the two types of regions.

The advantage of the MFM is that it is not as sensitive to surface contamination, roughness or disorder as the STM. Even 5–10 nm of contamination would be tolerable as long as it is not magnetic. This is because magnetic forces are long range. On the other hand, this also means that the MFM does not have as high resolution as the STM. The highest lateral resolution claimed for MFM is about 20 nm, or about one hundred times worse than the STM. Nevertheless, the resolu-

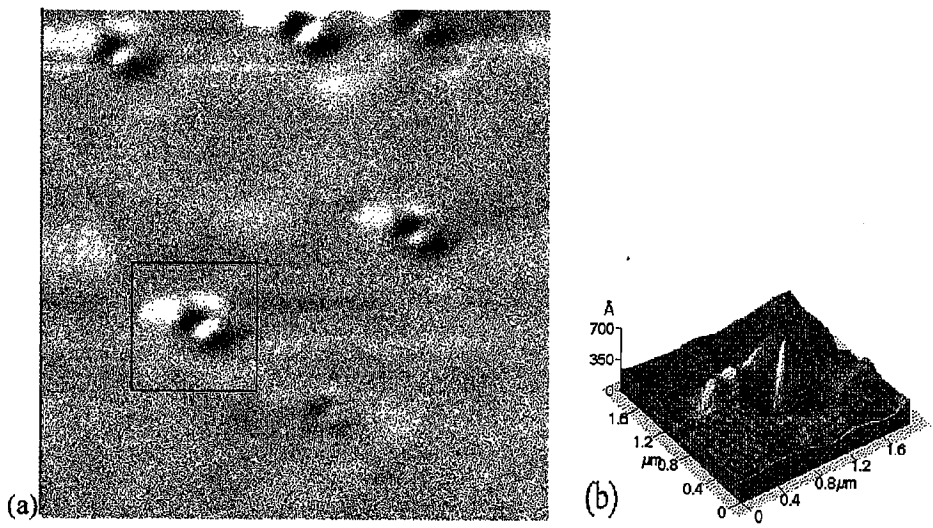

Fig. 6. (a) Noncontact LT MFM image, 6.1 μm on a side, of a $YBa_2Cu_3O_{7-x}$ film showing vortices with an asymmetric shape. The gray scale spans 61 nm. (b) 3D display of the vortex marked in (a). Reproduced from Ref. [21].

tion is sufficient to study interesting structures such as vortices at flux penetration through weak portions the superconductor. An example of a vortex is shown in Fig. 6.

5. Conclusion

There are far more scanning probe techniques that can be applied to superconductors. For example, one can use as a probe a small SQUID coil, a small Hall bar, or a near field tip for optical or microwave frequencies. Each technique has strengths and weaknesses. A broad knowledge of these techniques is ideal in order to choose the best tool to solve a particular problem. Fortunately much of the scanning electronics and computer control, as well as the troubleshooting of imaging artifacts, are common to all. Therefore the "Swiss Army knife" of scanning probe techniques should be in every scientists' pocket.

Acknowledgments

The authors are pleased to gratefully acknowledge the supporting agencies and collaborators who have made this research possible. This work has been supported over the years by the National Science Foundation, the Texas Advanced and Technology Programs, and the R.A. Welch Foundation. Many people have collaborated with the authors in the work reviewed here, most notably those at the University of Texas (at the time the research was done): Alex Barr, Chun-Che Chen, David Derro, Qingyou Lu, and Shuheng H. Pan. The first author benefited from recent conversations with S.H. Pan on the artifacts that are possible in spectroscopic measurements.

References

[1] E.L. Wolf, *Principles of Tunneling Spectroscopy*, Oxford Univ. Press, New York 1985; *Tunneling Spectroscopy*, Ed. P.K. Hansma, Plenum, New York 1982.

[2] R.J. Hamers, R.M. Tromp, J.E. Demuth, *Phys. Rev. Lett.* **56**, 1972 (1986).

[3] R.M. Feenstra, J.A. Stroscio, *Phys. Rev. Lett.* **59**, 2173 (1987).

[4] A.L. de Lozanne, in: *Investigations of Surfaces and Interfaces - Part A*, Eds. B.W. Rossiter, R.C. Baetzold, Review chapter for Physical Methods of Chemistry Series, 2nd ed., Vol. IXA, John Wiley, New York 1993, p. 141, 48 figures.

[5] S.A. Elrod, A. de Lozanne, C.F. Quate, *Appl. Phys. Lett.* **45**, 1240 (1984).

[6] A.L. de Lozanne, S.A. Elrod, C.F. Quate, *Phys. Rev. Lett.* **54**, 2433 (1985).

[7] S. Pan, K.W. Ng, A.L. de Lozanne, J.M. Tarascon, L.H. Greene, *Phys. Rev. B* **35**, 7220 (1987).

[8] A.L. de Lozanne, E. Ogawa, R.M. Silver, A.B. Berezin, S. Pan, in: *Science and Technology of Thin Film Superconductors*, Eds. R.D. McConnel, S.A. Wolf, Plenum Press, New York 1988, p. 111.

[9] A.L. de Lozanne, S.H. Pan, H.L. Edwards, D.J. Derro, A.L. Barr, J.T. Markert, *SPIE* **2696**, 347 (1996).

[10] S.H. Pan, Ph.D. Thesis, University of Texas, 1991, unpublished.

[11] H.L. Edwards, J.T. Markert, A.L. de Lozanne, *J. Vac. Sci. Tech. B* **12**, 1886 (1994).

[12] H.L. Edwards, A.L. Barr, J.T. Markert, A.L. de Lozanne, *Phys. Rev. Lett.* **73**, 1154 (1994).

[13] H.A. Mook, P. Dai, K. Salama, D. Lee, F. Dogan, G. Aeppli, A.T. Boothroyd, *Phys. Rev. Lett.* **77**, 370 (1996).

[14] H.L. Edwards, J.T. Markert, A.L. de Lozanne, *Phys. Rev. Lett.* **69**, 2967 (1992).

[15] J. Tersoff, D.R. Hamann, *Phys. Rev. Lett.* **50**, 1998 (1983); *Phys. Rev. B* **31**, 805 (1985).

[16] H.L. Edwards, D.J. Derro, A.L. Barr, J.T. Markert, A.L. de Lozanne, *Phys. Rev. Lett.* **75**, 1387 (1995).

[17] V.Z. Kresin, S.A. Wolf, *Phys. Rev. B* **51**, 1229 (1995).

[18] A.H. Castro Neto, *Phys. Rev. Lett.* **78**, 3931 (1997).

[19] G. Binnig, H. Rohrer, *Helv. Phys. Acta* **55**, 726 (1982); G. Binnig, H. Rohrer, Ch. Gerber, E. Weibel, *Phys. Rev. Lett.* **50**, 120 (1983).

[20] P.J.M. van Bentum, R.T.M. Smokers, H. van Kempen, *Phys. Rev. Lett.* **60**, 2543 (1988).

[21] C.W. Yuan, E. Batalla, A. deLozanne, M. Kirk, M. Tortonese, *Appl. Phys. Lett.* **65**, 1308 (1994).

[22] C.W. Yuan, Z. Zheng, A.L. de Lozanne, M. Tortonese, D.A. Rudman, J.N. Eckstein, *J. Vac. Sci. Technol. B* **14**, 1210 (1996).

[23] H.L. Edwards, D.J. Derro, A.L. Barr, J.T. Markert, A.L. de Lozanne, *J. Vac. Sci. Technol. B* **14**, 1217 (1996).

[24] D.J. Derro, T. Koyano, H. Edwards, A. Barr, J.T. Markert, A.L. de Lozanne, in: *Proc. 10th Anniversary HTS Workshop on Physics, Materials and Applications*, Eds. B. Batlogg, C.W. Chu, W.K. Chu, D.U. Gubser, K.A. Müller, World Scientific, Singapore 1996, p. 433.